Effects of time-dependent ATP consumption caused by neuron firing on ATP concentrations in synaptic boutons containing and lacking a stationary mitochondrion

Andrey V. Kuznetsov

Department of Mechanical and Aerospace Engineering, North Carolina State University,

Raleigh, NC 27695-7910, USA; e-mail: avkuznet@ncsu.edu

Abstract

The reason why only about half of the presynaptic release sites lack a stationary mitochondrion, and how the sites without a stationary mitochondrion are supplied with ATP, is still not fully understood. This paper develops a mathematical model designed to simulate the transient ATP concentration in presynaptic en passant boutons. The model is utilized to investigate how the ATP concentration responds to increased ATP demand during neuronal firing in boutons with a stationary mitochondrion and those without one. The analysis suggests that neuron firing may cause oscillations in the ATP concentrations, with peak-to-peak amplitudes ranging from 0.4% to 5% of their average values. However, this does not deplete boutons lacking a mitochondrion of ATP; their concentration remains approximately 3.75 times higher than the minimum concentration required for synaptic activity. The variance in average ATP concentrations between boutons containing a stationary mitochondrion and those lacking one ranges from 0.3% to 0.8%, contingent on the distance between the boutons. The model indicates that diffusion-driven ATP transport is rapid enough to adequately supply ATP molecules to boutons lacking a stationary mitochondrion.

Keywords: axons; mitochondria; ATP; diffusion-driven transport; computational modeling

Abbreviations

CV control volume

PDE partial differential equation

1. Introduction

The main role of mitochondria is to produce easily accessible chemical energy in the form of ATP [1,2]. This occurs because mitochondrial respiration generates a substantially larger amount of ATP from a glucose molecule compared to glycolysis, with a ratio of 36:2.

Apart from stationary mitochondria, there are also mitochondria that are transported in anterograde and retrograde directions [3-6]. These mobile mitochondria contribute to supplying ATP to energy-demanding sites, such as en passant boutons (hereafter referred to as boutons). However, it is believed that the primary source of ATP for these boutons comes from stationary mitochondria that specifically dock in them [7-9].

In the brain, synapses represent the main locations where ATP is consumed [10]. The reason why only about half of the presynaptic release sites contain a stationary mitochondrion remains a mystery, while the remaining sites lack one [11-14]. The question of how a bouton without a stationary mitochondrion obtains its supply of ATP is investigated in this paper.

Three competing hypotheses in the literature propose explanations for this phenomenon: ATP is transported to boutons lacking mitochondria through diffusion [15], ATP is synthesized in boutons lacking mitochondria via glycolysis [15], and ATP needs are partially fulfilled by ATP production in neighboring axons, dendrites, and glial cells [12,16].

Choosing among these three models requires investigating whether diffusion-driven ATP transport is sufficiently fast to support ATP demand in a bouton lacking a mitochondrion. If diffusion is fast enough, the ATP concentration will remain relatively uniform; if it is slow, the ATP concentration will decrease with distance from a mitochondrion and fall below the threshold needed to sustain synaptic activity in a bouton lacking a mitochondrion [12,16].

Compartmental models are frequently employed in synapse modeling. Ref. [17] developed a model comprising 33 ordinary differential equations, which simulates neuronal, astrocytic, extracellular, and vascular compartments. In [18], a neurochemical model of a tripartite synapse was developed, which involves 143 ordinary differential equations. This model predicts the occurrence of local sleep, crucial for cellular resource restoration.

Unlike previous models, the model developed here tracks not only ATP variation over time but also over position in the axon. This allows for simulating differences in ATP concentration between synapses with and without a stationary mitochondrion. In contrast to our previous work [19], which solely simulated a

steady-state scenario, this study simulates a scenario where ATP consumption fluctuates due to neuron firing.

The frequency of neuron firing usually falls within the range of 1 to 200 Hz [20]. The rate of ATP production by mitochondria fluctuates over the course of the day [21]. However, mitochondria are unlikely to adjust ATP production at a pace equivalent to neuron firing. According to ref. [22], the estimated response time for mitochondrial oxygen consumption to stepwise changes in cardiac energy demand is 4-8 seconds. Ref. [23] suggests that it takes minutes to change the ATP production rate in mitochondria. The significant reliance on glycolysis for ATP production during high-intensity exercise, as noted in ref. [24], implies that ATP production by mitochondria cannot be increased within seconds. Considering that ATP cannot be stored and must be generated as needed [25], it is reasonable to ask about the extent of ATP concentration variations in boutons due to changes in ATP demand during neuron firing.

2. Materials and models

2.1. Equations governing ATP concentration in a single periodic unit control volume (CV) containing a bouton having a stationary mitochondrion and a bouton lacking a stationary mitochondrion

In developing the model, it was postulated that a stationary mitochondrion is present at the center of every other varicosity (bouton) along the axon. This simplifying assumption of periodicity enabled the definition of a periodic unit CV containing half of a mitochondrion (the other half belonging to a neighboring periodic CV), as illustrated in Fig. 1. The width of axonal varicosity is denoted by 2δ, while the average spacing between varicosities is denoted by L. Stationary mitochondria are assumed to be present at every second varicosity, with a distance of $2L + 4\delta$ between them.

In the segment of the varicosity where a stationary mitochondrion is located (Fig. 1), the conservation of ATP molecules leads to the following equation:

$$\frac{\partial C_1}{\partial t} = D\frac{\partial^2 C_1}{\partial x^2} - aC_1 + m\,, \qquad 0 \le x \le x_m\,, \tag{1}$$

where t denotes the time and x denotes the linear coordinate along the axon. Eq. (1) assumes that ATP consumption is proportional to the amount of ATP available for binding.

In the segment of varicosity not occupied by a stationary mitochondrion (Fig. 1), the conservation equation for ATP molecules is as follows:

$$\frac{\partial C_2}{\partial t} = D\frac{\partial^2 C_2}{\partial x^2} - aC_2 , \quad x_m \le x \le \delta . \tag{2}$$

In the space between varicosities, known as intervaricosity spacing (Fig. 1), the conservation of ATP leads to the following equation:

$$\frac{\partial C_3}{\partial t} = D\frac{\partial^2 C_3}{\partial x^2} , \delta \le x \le \delta + L . \tag{3}$$

In an empty varicosity, where ATP is still consumed, but which does not contain a stationary mitochondrion (Fig. 1), the conservation of ATP yields the following equation, which is similar to Eq. (2):

$$\frac{\partial C_4}{\partial t} = D\frac{\partial^2 C_4}{\partial x^2} - aC_4 , \quad L + \delta \le x \le L + 2\delta . \tag{4}$$

The only dependent variable in the model is the linear concentration of ATP in the axon, denoted as *C*. The model parameters are summarized in Table 1.

Given that a significant portion (~80%) of energy in mammalian cortex neurons is expended on action potentials [26], it is anticipated that ATP consumption will fluctuate over time. In order to simulate the fluctuating ATP consumption rate needed to sustain synaptic activity during neuronal firing, the following periodic ATP consumption rate is assumed:

$$a = a_0 \left(1 + \text{square}(2\pi f t)\right) , \tag{5}$$

where $\text{square}(2\pi f t)$ is a periodic step function with a period of $T = \frac{1}{f}$. It resembles the sine function but produces a square wave with values of –1 and 1.

Fig. 2 illustrates the function $1 + \text{square}(2\pi f t)$ for *f*=1 Hz during the initial 10 seconds. Eq. (5) follows an all-or-nothing approximation. A basal level of ATP consumption is necessary in a synapse for homeostatic maintenance [27]. However, as the objective of this paper is to estimate the maximum amplitude of ATP concentration oscillations in boutons with and without a stationary mitochondrion in response to neuron firing, the approximation given by Eq. (5) is justified.

Eqs. (1)-(4) were solved with the following boundary conditions:

$$\text{At } x = 0 : \qquad \left.\frac{\partial C_1}{\partial x}\right|_{x=0} = 0 . \tag{6}$$

At $x = x_m$: $$C_1\big|_{x=x_m-0} = C_2\big|_{x=x_m+0}, \; D\frac{\partial C_1}{\partial x}\bigg|_{x=x_m-0} = D\frac{\partial C_2}{\partial x}\bigg|_{x=x_m+0}. \tag{7a,b}$$

At $x = \delta$: $$C_2\big|_{x=\delta-0} = C_3\big|_{x=\delta+0}, \; D\frac{\partial C_2}{\partial x}\bigg|_{x=\delta-0} = D\frac{\partial C_3}{\partial x}\bigg|_{x=\delta+0}. \tag{8a,b}$$

At $x = L + \delta$: $$C_3\big|_{x=L+\delta-0} = C_4\big|_{x=L+\delta+0}, \; D\frac{\partial C_3}{\partial x}\bigg|_{x=L+\delta-0} = D\frac{\partial C_4}{\partial x}\bigg|_{x=L+\delta+0}. \tag{9a,b}$$

At $x = L + 2\delta$: $$\frac{\partial C_4}{\partial x}\bigg|_{x=L+2\delta} = 0. \tag{10}$$

ATP diffusivity is incorporated into the left- and right-hand sides of Eqs. (7b), (8b), and (9b) to allow for potential model extensions in the future. This allows for the possibility of different diffusivity values in different subdomains.

Zero initial conditions were employed:

At $t = 0$: $$C_1 = 0, \; C_2 = 0, \; C_3 = 0, \; C_4 = 0. \tag{11}$$

Table 1. Parameters describing ATP transport and accumulation in the axon.

Symbol	Definition	Units	Value or range	Reference(s)	Value used in computations
a_0	Kinetic constant describing the rate of ATP consumption in a bouton	s^{-1}	0.23 [a]		0.23
A_c	Cross-sectional area of an axon	μm^2	0.79 [b]		0.79
C_0	Linear ATP concentration in the axon	μm^{-1}	1.42×10^6 [c]	[15]	1.42×10^6
$\hat{C}_0$	Volumetric ATP concentration in the axon	mM	2-4	[15]	3
$C_{\min}$	Minimum linear ATP concentration needed to	μm^{-1}	3.78×10^5 [d]	[15]	3.78×10^5

	support synaptic transmission				
D	Diffusivity of ATP in the cytosol	$\mu m^2\ s^{-1}$	$710-720$ in water, ~300 in the cytosol	[28,29]	300
f	Frequency at which neuron fires	Hz	1-200	[20]	1, 10
L	Average spacing between varicosities	μm	3	[12]	3, 10
m	Rate of ATP production per unit length of a mitochondrion	$\mu m^{-1}s^{-1}$	1.85×10^5 [e]	[30-32]	1.29×10^6
$\dot{m}$	Rate of ATP production per unit mass of tissue	mol/(s kg)	1.1×10^{-4} -1.83×10^{-4} [f]	[30]	1.33×10^{-4}
$2x_m$	Length of a mitochondrion	μm	0.5-10	Fig. 2G of [12], [33]	1
γ	Percent of mitochondria by volume in tissues	%	2-10	[32]	5
δ	Half-width of axonal varicosity	μm	1	Fig. 2E of [12], [34]	1
ϖ	Mass of a single mitochondrion	kg	322×10^{-15}	[31]	322×10^{-15}

[a] The value of a_0 was found by using the analytical solution given in section S1 of Supplementary Materials. The condition used was that the maximum value of ATP concentration at a constant rate of ATP consumption in boutons, occurring at $x=0$, is equal to C_0.

[b] The estimation of A_c proceeded as follows:

$A_c = \frac{\pi d^2}{4}$. A diameter of 1 μm was used for the axon diameter, *d*. Cross-sectional area A_c was assumed to be constant in our model.

[c] This value was estimated as follows:

$C_0 = \hat{C}_0 \times 10^{-18} N_A A_c$ ATP/ μm.

[d] To sustain synaptic transmission, boutons must sustain a minimum ATP concentration of around 0.8 mM [15]. This corresponds to

$C_{\min} = 0.8 \times 10^{-18} N_A A_c = 3.78 \times 10^5$ ATP/μm.

[e] The quantity of ATP molecules produced by mitochondria per unit length of the axon is approximated as:

$m = \varpi(\gamma / 100\%)\dot{m} N_A / (2x_m)$.

[f] The range for $\dot{m}$ given in ref. [30] is between 6.6×10^{-3}-11×10^{-3} mol/(min kg).

2.2. Numerical solution

Eqs. (1)-(4) constitute a system of partial differential equations (PDEs) that can be solved by a single-domain approach [35]. This method employs a single PDE, with coefficients that change at subdomain interfaces. As a result, the equation adjusts to the appropriate form within each of the four subdomains:

$$\frac{\partial C}{\partial t} = D\frac{\partial^2 C}{\partial x^2} - \hat{a}C + \hat{m}\,, \tag{12}$$

where

$$\hat{a} = a\,,\quad \hat{m} = m\,,\qquad 0 \le x \le x_m\,, \tag{13a}$$

$$\hat{a} = a\,,\ \hat{m} = 0\,,\qquad x_m \le x \le \delta\,, \tag{13b}$$

$$\hat{a} = 0\,,\ \hat{m} = 0\,,\qquad \delta \le x \le \delta + L\,, \tag{13c}$$

$$\hat{a} = a\,,\ \hat{m} = 0\,,\qquad L + \delta \le x \le L + 2\delta\,. \tag{13d}$$

As Eq. (12) applies throughout the entire computational domain, only boundary conditions at external boundaries, $x = 0$ and $x = L + 2\delta$, are necessary:

$$\text{At } x = 0: \quad \left.\frac{\partial C}{\partial x}\right|_{x=0} = 0 . \tag{14}$$

$$\text{At } x = L + 2\delta: \quad \left.\frac{\partial C}{\partial x}\right|_{x=L+2\delta} = 0 . \tag{15}$$

Employing the single-domain approach yields a numerical solution that automatically satisfies the continuity of the ATP concentration and ATP flux across the interfaces between subdomains, $x = x_m$, $x = \delta$, and $x = \delta + L$. This means that Eqs. (7)-(9) are satisfied automatically.

Eq. (12) is solved with the following initial condition:

$$\text{At } t = 0: \quad C = 0 . \tag{16}$$

Eq. (12), along with boundary conditions given by Eqs. (14) and (15), and initial condition (16), was solved using a well-validated MATLAB's PDEPE solver (MATLAB R2023a, MathWorks, Natick, MA, USA). For f=1 Hz, a (100,10000) mesh was employed in the (x,t) domain, while for f=10 Hz, a (100,100000) mesh was used. At a frequency of 10 Hz, the computational time on a PC with an Intel Core i9 processor was approximately 6 hours, which is due to a large number of oscillations in ATP consumption rate imposed to simulate neuronal firing.

3. Results

Figs. 3-5 show the results for L=3 μm and f=1 Hz. To check the accuracy of the numerical solution for ATP concentration, it was compared with the analytical solution obtained in ref. [19] for the scenario involving a constant rate of ATP consumption in a bouton ($a = a_0 =$ constant). For the paper to be self-contained, this solution is provided in Section S1 of the Supplementary Materials. Both the numerical and analytical solutions are identical (Fig. 3).

Oscillations in the ATP consumption rate caused by neuronal firing led to small oscillations in ATP concentrations in boutons. The peak-to-peak amplitude of these oscillations is approximately 5% of their average value (Fig. 4, Table 2). The ATP concentration in a bouton lacking a stationary mitochondrion oscillates in a manner similar to that in a bouton having a stationary mitochondrion, but the average concentration is approximately 0.3% lower (Fig. 4b, Table 3). However, due to the small amplitude of these oscillations, they are unable to reduce the ATP concentration in a bouton lacking a stationary

mitochondrion below the threshold required to sustain synaptic activity (3.78×10^5 ATP/μm, as shown in Table 1). This is explained by the high diffusivity of ATP (300 $\mu m^2\ s^{-1}$, see Table 1). The oscillations shown in Fig. 4 are consistent with the ATP concentration oscillations reported in ref. [18].

At a given time, the ATP concentration decreases from the center of the bouton containing a stationary mitochondrion to the center of the bouton without a stationary mitochondrion (Fig. 5). The decrease in ATP concentration displayed in Fig. 5 qualitatively agrees with the decrease in the ATP:ADP signal ratio as the distance from a mitochondrion increases, as reported in Fig. 4E of ref. [36]. The difference in ATP concentrations between the bouton containing a stationary mitochondrion and the bouton lacking a stationary mitochondrion is only 0.3% of the average value (Fig. 5, Table 3). This may explain why ref. [37] observed a uniform ATP/ADP ratio along an axon.

The concentration at the center of the bouton without a stationary mitochondrion (at x=5 μm) is 3.85 times higher than the minimum ATP concentration given in Table 1. This estimate is consistent with the one given in ref. [19], where we reported a ratio of 3.75 for the scenario involving a constant ATP consumption rate. When an oscillating ATP consumption rate, as described by Eq. (5), is taken into account, the ATP concentration is 2.5% higher compared to the scenario with a constant ATP consumption rate (Fig. 5, Table 4).

Table 2. The peak-to-peak amplitude of oscillations of the ATP concentrations because of neuron firing, percentage of the average value.

	L=3 μm	L=10 μm
f=1 Hz	5%	2%
f=10 Hz	0.5%	0.4%

Table 3. The percentage by which the average ATP concentration in a bouton lacking a stationary mitochondrion is lower than that in a bouton having a stationary mitochondrion.

	L=3 μm	L=10 μm
f=1 Hz	0.3%	0.8%
f=10 Hz	0.4%	0.6%

Table 4. The percentage by which the average ATP concentration for the oscillating ATP consumption rate, described by Eq. (5), is higher than the average ATP concentration for a constant ATP consumption rate, a_0 (Table 1).

	L=3 μm	L=10 μm
f=1 Hz	2.5%	1%
f=10 Hz	0.3%	0.2%

Increasing the frequency of neuron firing from 1 Hz to 10 Hz leads to a reduction in the peak-to-peak amplitude of ATP concentration oscillations, which is now 0.5% of the average value, as shown in Fig. S1b in the Supplementary Materials (also see Table 2). The average ATP concentration in a bouton lacking a stationary mitochondrion is approximately 0.4% lower than that in a bouton containing a stationary mitochondrion (Fig. S1b and Table 3). The ATP concentration for the scenario with an oscillating ATP consumption rate is approximately 0.3% higher than that for the scenario with a constant ATP consumption rate (Fig. S2 and Table 4).

Given that pathological increases in the distance between mitochondria could lead to local energy failure in boutons [15], the scenario with L=10 μm and f=1 Hz was examined in Figs. 6 and 7. The ATP concentration in a bouton lacking a stationary mitochondrion oscillates similarly to that in a bouton containing a stationary mitochondrion, but the average concentration is approximately 0.8% lower (Fig. 7 and Table 3). The increased difference in ATP concentrations between boutons with and without a stationary mitochondrion (previously 0.3% in Fig. 5, see also Table 3) is attributed to diffusion-driven transport of ATPs over a greater distance. The peak-to-peak amplitude of ATP concentration oscillations in boutons with and without a stationary mitochondrion is approximately 2% of their average values (Fig. 6b and Table 2). This is lower than in Fig. 4b. Increasing the distance between the boutons appears to decrease the amplitude of ATP concentration oscillations.

The difference in ATP concentration between a bouton containing a stationary mitochondrion and a bouton lacking a stationary mitochondrion is 0.8% (Fig. 7 and Table 3), which is higher than the 0.3% difference observed for the case of L=3 μm (Fig. 5, see also Table 3). The ATP concentration in a bouton lacking a stationary mitochondrion remains 3.75 times higher than the minimum ATP concentration required to sustain synaptic activity (3.78×10^5 ATP/μm). The ATP concentration for the oscillating ATP consumption rate, described by Eq. (5), is approximately 1% higher than that for a constant ATP consumption rate, a_0 (Fig. 7 and Table 4). Note that the difference in ATP concentrations between the

scenarios with oscillating and constant ATP consumption diminishes as the distance between the boutons increases. In the corresponding scenario in Fig. 5, this difference was 2.5%, see also Table 4.

Increasing the frequency of neuron firing from 1 Hz to 10 Hz results in a reduced peak-to-peak amplitude of ATP concentration oscillations (0.4%, as shown in Fig. S3b, see also Table 2). The average ATP concentration in a bouton lacking a stationary mitochondrion is approximately 0.6% lower than that in a bouton containing a stationary mitochondrion (Fig. S4, see also Table 3). When considering an oscillating ATP consumption rate, the ATP concentration is approximately 0.2% higher compared to when assuming a constant ATP consumption rate (Fig. S4 and Table 4).

4. Discussion, limitations of the model, and future directions

The study examined ATP concentration oscillations in boutons triggered by neuron firing. The peak-to-peak amplitudes of these oscillations ranged from 0.4% to 5% of their average values, depending on the intervaricosity spacing and on the frequency of neuron firing (Table 2). The increase in intervaricosity spacing and frequency of neuron firing decreases the amplitude of oscillations of the ATP concentration. The oscillations are observed to be similar in boutons containing and lacking a stationary mitochondrion.

Diffusion-driven transport necessitates concentration gradients, requiring an ATP gradient between boutons with and without a stationary mitochondrion. Results indicate a 0.3% to 0.8% lower ATP concentration in boutons lacking stationary mitochondria (Table 3). The increase in intervaricosity spacing increases the difference in ATP concentrations between boutons containing and lacking a stationary mitochondrion. However, the ATP concentration in these boutons remains 3.75 times higher than that needed for synaptic activity, suggesting that having a stationary mitochondrion in every bouton is not necessary. With a mitochondrion present in every second bouton, ATP diffusion maintains sufficient ATP concentration levels, avoiding significant concentration drops in boutons lacking mitochondria.

When considering an oscillating ATP consumption rate, the ATP concentration is 0.2% to 2.5% higher compared to that assuming a constant ATP consumption rate (Table 4). The increase in intervaricosity spacing and frequency of neuron firing decreases the difference in ATP concentrations between scenarios with oscillating and constant ATP consumption rates.

The model's limitations stem from assuming a constant rate of ATP production by mitochondria and neglecting ATP production by glycolysis. Future research should aim to develop more comprehensive

models of biochemical processes within synapses and mitochondria to better simulate ATP production and consumption rates.

Acknowledgment

AVK acknowledges the support provided by the National Science Foundation (grant CBET-2042834) and the Alexander von Humboldt Foundation through the Humboldt Research Award.

References

[1] Fan, T. J., Xia, L., and Han, Y. R., 2001, "Mitochondrion and Apoptosis," Acta Biochimica Et Biophysica Sinica, **33**(1), pp. 7-12.

[2] Picard, M., and McEwen, B. S., 2018, "Psychological Stress and Mitochondria: A Systematic Review," Psychosomatic Medicine, **80**(2), pp. 141-153.

[3] Mogre, S. S., Brown, A., I., and Koslover, E. F., 2020, "Getting Around the Cell: Physical Transport in the Intracellular World," Physical Biology, **17**(6), pp. 061003.

[4] Melkov, A., and Abdu, U., 2018, "Regulation of Long-Distance Transport of Mitochondria Along Microtubules," Cellular and Molecular Life Sciences, **75**(2), pp. 163-176.

[5] Kruppa, A. J., and Buss, F., 2021, "Motor Proteins at the Mitochondria Cytoskeleton Interface," Journal of Cell Science, **134**(7), pp. jcs226084.

[6] Narayanareddy, B. R. J., Vartiainen, S., Hariri, N., 2014, "A Biophysical Analysis of Mitochondrial Movement: Differences between Transport in Neuronal Cell Bodies Versus Processes," Traffic, **15**(7), pp. 762-771.

[7] Hollenbeck, P. J., and Saxton, W. M., 2005, "The Axonal Transport of Mitochondria," Journal of Cell Science, **118**(23), pp. 5411-5419.

[8] Lees, R. M., Johnson, J. D., and Ashby, M. C., 2020, "Presynaptic Boutons that Contain Mitochondria are More Stable," Frontiers in Synaptic Neuroscience, **11**, pp. 37.

[9] Lewis, T. L., Jr., Turi, G. F., Kwon, S., 2016, "Progressive Decrease of Mitochondrial Motility during Maturation of Cortical Axons in Vitro and in Vivo," Current Biology, **26**(19), pp. 2602-2608.

[10] Harris, J. J., Jolivet, R., and Attwell, D., 2012, "Synaptic Energy Use and Supply," Neuron, **75**(5), pp. 762-777.

[11] Obashi, K., and Okabe, S., 2013, "Regulation of Mitochondrial Dynamics and Distribution by Synapse Position and Neuronal Activity in the Axon," European Journal of Neuroscience, **38**(3), pp. 2350-2363.

[12] Shepherd, G., and Harris, K. M., 1998, "Three-Dimensional Structure and Composition of CA3 -> CA1 Axons in Rat Hippocampal Slices: Implications for Presynaptic Connectivity and Compartmentalization," Journal of Neuroscience, **18**(20), pp. 8300-8310.

[13] Chang, D. T. W., Honick, A. S., and Reynolds, I. J., 2006, "Mitochondrial Trafficking to Synapses in Cultured Primary Cortical Neurons," Journal of Neuroscience, **26**(26), pp. 7035-7045.

[14] Yang, S., Park, J. H., and Lu, H., 2023, "Axonal Energy Metabolism, and the Effects in Aging and Neurodegenerative Diseases," Molecular Neurodegeneration, **18**(1), pp. 49.

[15] Pathak, D., Shields, L. Y., Mendelsohn, B. A., 2015, "The Role of Mitochondrially Derived ATP in Synaptic Vesicle Recycling," Journal of Biological Chemistry, **290**(37), pp. 22325-22336.

[16] Engl, E., and Attwell, D., 2015, "Non-Signalling Energy use in the Brain," Journal of Physiology-London, **593**(16), pp. 3417-3429.

[17] Jolivet, R., Coggan, J. S., Allaman, I., 2015, "Multi-Timescale Modeling of Activity-Dependent Metabolic Coupling in the Neuron-Glia-Vasculature Ensemble," PLOS Computational Biology, **11**(2), pp. e1004036.

[18] Joshi, S. N., Joshi, A. N., and Joshi, N. D., 2023, "Interplay between Biochemical Processes and Network Properties Generates Neuronal Up and Down States at the Tripartite Synapse," Physical Review E, **107**(2), pp. 024415.

[19] Kuznetsov, I. A., and Kuznetsov, A. V., 2023, "ATP Diffusional Gradients are Sufficient to Maintain Bioenergetic Homeostasis in Synaptic Boutons Lacking Mitochondria," International Journal for Numerical Methods in Biomedical Engineering, **39**(5), pp. e3696.

[20] Barraza, D., Kita, H., and Wilson, C. J., 2009, "Slow Spike Frequency Adaptation in Neurons of the Rat Subthalamic Nucleus," Journal of Neurophysiology, **102**(6), pp. 3689-3697.

[21] Weinrich, T. W., Kam, J. H., Ferrara, B. T., 2019, "A Day in the Life of Mitochondria Reveals Shifting Workloads," Scientific Reports, **9**(1), pp. 13898.

[22] van Beek, J. H., and Westerhof, N., 1990, "Response Time of Mitochondrial Oxygen Consumption Following Stepwise Changes in Cardiac Energy Demand," Advances in Experimental Medicine and Biology, **277**, pp. 415-423.

[23] Picard, M., McEwen, B. S., Epel, E. S., 2018, "An Energetic View of Stress: Focus on Mitochondria," Frontiers in Neuroendocrinology, **49**, pp. 72-85.

[24] Calbet, J. A. L., Martín-Rodríguez, S., Martin-Rincon, M., 2020, "An Integrative Approach to the Regulation of Mitochondrial Respiration during Exercise: Focus on High-Intensity Exercise," Redox Biology, **35**, pp. 101478.

[25] Pizzorno, J., 2014, "Mitochondria-Fundamental to Life and Health," Integrative Medicine (Encinitas, Calif.), **13**(2), pp. 8-15.

[26] Lennie, P., 2003, "The Cost of Cortical Computation," Current Biology, **13**(6), pp. 493-497.

[27] Rangaraju, V., Calloway, N., and Ryan, T. A., 2014, "Activity-Driven Local ATP Synthesis is Required for Synaptic Function," Cell, **156**(4), pp. 825-835.

[28] Bowen, W. J., and Martin, H. L., 1964, "The Diffusion of Adenosine Triphosphate through Aqueous Solutions," Archives of Biochemistry and Biophysics, **107**(1), pp. 30-36.

[29] Macdonald, C. L., Yu, D., Buibas, M., 2008, "Diffusion Modeling of ATP Signaling Suggests a Partially Regenerative Mechanism Underlies Astrocyte Intercellular Calcium Waves," Frontiers in Neuroengineering, **1**, pp. 1.

[30] Wibom, R., and Hultman, E., 1990, "Atp Production-Rate in Mitochondria Isolated from Microsamples of Human Muscle," American Journal of Physiology, **259**(2), pp. E204-E209.

[31] Fuchs, P., Rugen, N., Carrie, C., 2020, "Single Organelle Function and Organization as Estimated from Arabidopsis Mitochondrial Proteomics," Plant Journal, **101**(2), pp. 420-441.

[32] Willingham, T. B., Ajayi, P. T., and Glancy, B., 2021, "Subcellular Specialization of Mitochondrial Form and Function in Skeletal Muscle Cells," Frontiers in Cell and Developmental Biology, **9**, pp. 757305.

[33] Trushina, E., 2016, "A Shape Shifting Organelle: Unusual Mitochondrial Phenotype Determined with Three-Dimensional Electron Microscopy Reconstruction," Neural Regeneration Research, **11**(6), pp. 900-901.

[34] Agrawal, A., and Koslover, E. F., 2021, "Optimizing Mitochondrial Maintenance in Extended Neuronal Projections," PLOS Computational Biology, **17**(6), pp. e1009073.

[35] Kuznetsov, A. V., 2003, "Limitation of the Single-Domain Numerical Approach: Comparisons of Analytical and Numerical Solutions for a Forced Convection Heat Transfer Problem in a Composite Duct," Computer Assisted Mechanics and Engineering Sciences, **10**, pp. 33-43.

[36] Matsumoto, N., Hori, I., Kajita, M. K., 2022, "Intermitochondrial Signaling Regulates the Uniform Distribution of Stationary Mitochondria in Axons," Molecular and Cellular Neurosciences, **119**, pp. 103704.

[37] Zala, D., Hinckelmann, M., Yu, H., 2013, "Vesicular Glycolysis Provides on-Board Energy for Fast Axonal Transport," Cell, **152**(3), pp. 479-491.

Figure captions

Fig. 1. (a) A schematic diagram illustrating a single periodic unit CV containing half of a mitochondrion (with the other half belonging to a neighboring periodic CV). The width of axonal varicosity is denoted by 2δ ; the average spacing between varicosities is denoted by *L*. It is assumed that stationary mitochondria are positioned at every other varicosity. The spacing between stationary mitochondria is $2L + 4\delta$. *Figure generated with the aid of servier medical art, licensed under a creative commons attribution 3.0 generic license. http://Smart.servier.com.*

Fig. 2. A step function of time is employed to simulate the oscillation in the rate of ATP consumption in a bouton resulting from neuron firing, as described in Eq. (5), *f*=1 Hz. Only the first 10 seconds are depicted; thereafter, the pattern continues in the same manner until the end of the simulation ($t_f = 1000$ s).

Fig. 3. Comparison between the numerical results (this study) and the analytical solution obtained in ref. [19] for the linear ATP concentration in the axon, denoted as *C*, plotted against the distance from a stationary mitochondrion, *x*. Constant rate of ATP consumption in a bouton, *L*=3 μm.

Fig. 4. Variation with time of the linear ATP concentration at *x*=0 (at the center of a bouton with a stationary mitochondrion) and at $x = L + 2\delta$ (at the center of a bouton without a stationary mitochondrion). (a) The simulation covers the entire 1000 s. (b) The last 10 s of the simulation. *f*=1 Hz, *L*=3 μm.

Fig. 5. The variation of ATP concentration between the centers of two boutons, one containing a stationary mitochondrion (at *x*=0) and the other without a stationary mitochondrion (at $x = L + 2\delta$), at *t*=1000 s. *f*=1 Hz, *L*=3 μm. The numerical solution represents the case with oscillating ATP consumption (as per Eq. (5)), whereas the analytical solution corresponds to the scenario with constant ATP consumption, a_0 (given in Table 1).

Fig. 6. Variation with time of the linear ATP concentration at *x*=0 (at the center of a bouton with a stationary mitochondrion) and at $x = L + 2\delta$ (at the center of a bouton without a stationary mitochondrion). (a) The simulation covers the entire 1000 s. (b) The last 10 s of the simulation. *f*=1 Hz, *L*=10 μm.

Fig. 7. The variation of ATP concentration between the centers of two boutons, one containing a stationary mitochondrion (at *x*=0) and the other without a stationary mitochondrion (at $x = L + 2\delta$), at *t*=1000 s. *f*=1 Hz, *L*=10 μm. The numerical solution represents the case with oscillating ATP consumption

(as per Eq. (5)), whereas the analytical solution corresponds to the scenario with constant ATP consumption, a_0 (given in Table 1).

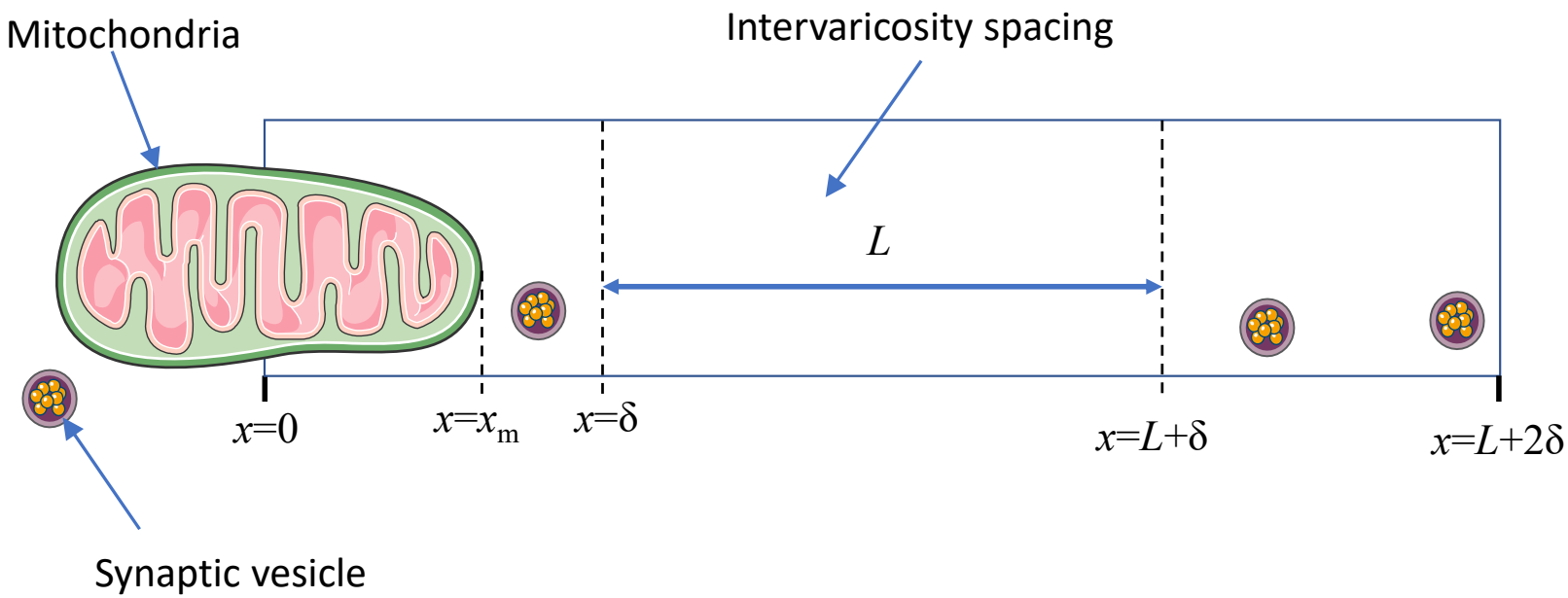
Mitochondria
Intervaricosity spacing
L
x=0
x=x_m
x=δ
x=L+δ
x=L+2δ
Synaptic vesicle

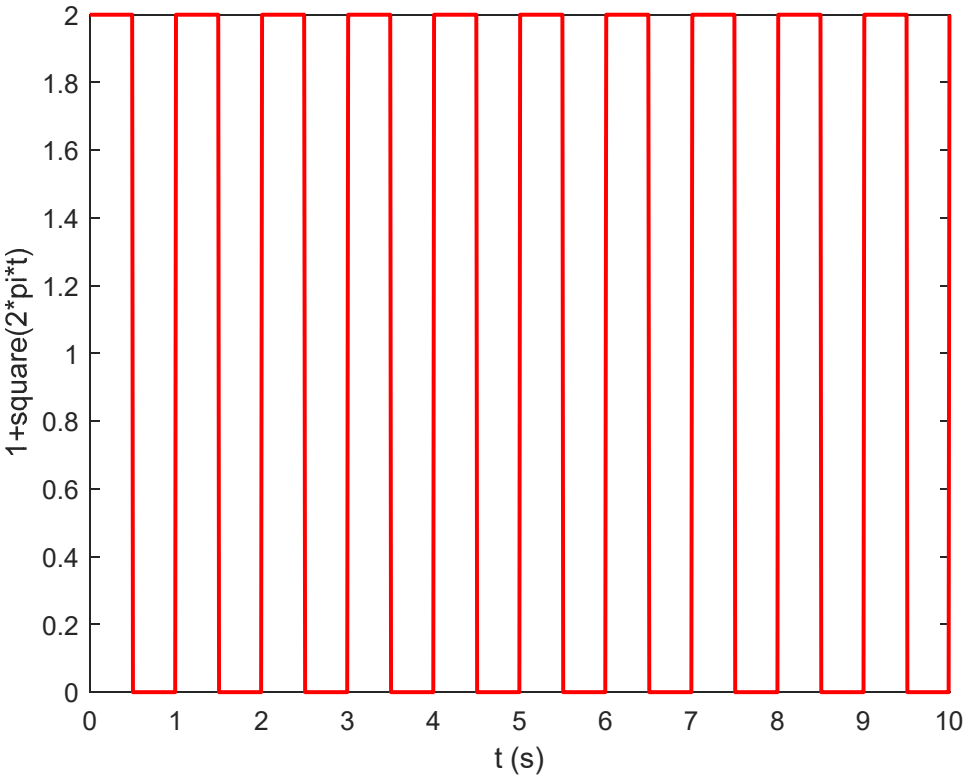

Figure 2

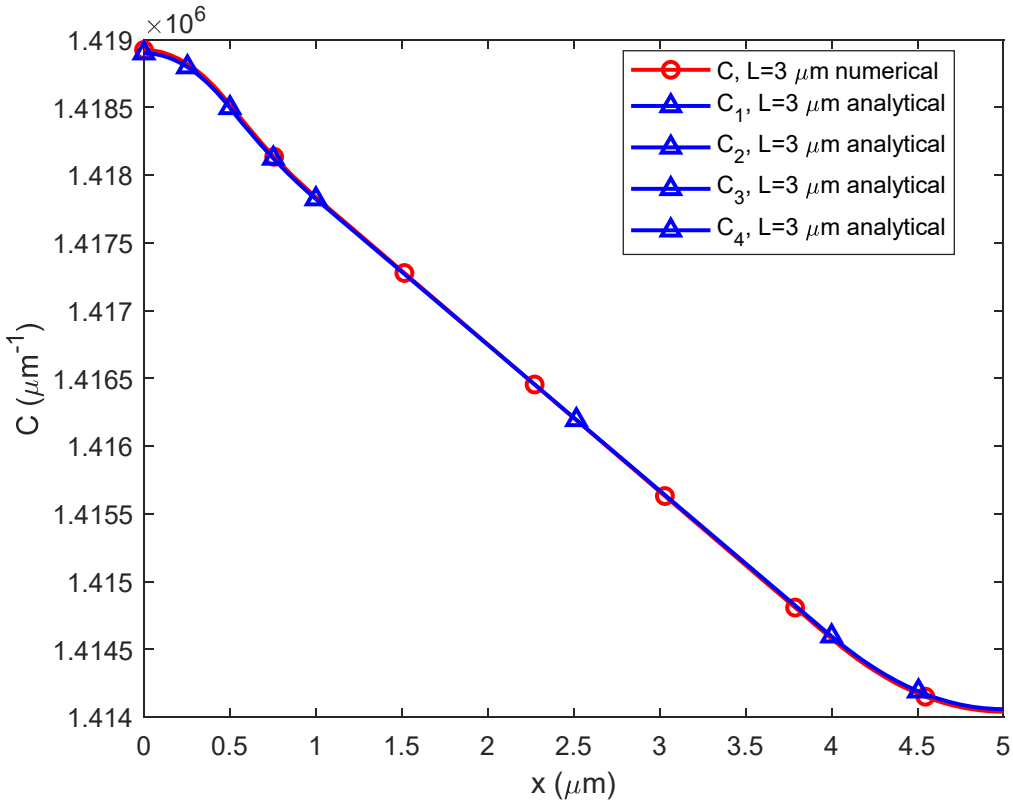
×10^6
1.419
1.4185
1.418
1.4175
1.417
1.4165
1.416
1.4155
1.415
1.4145
1.414
C (μm^-1)
0
0.5
1
1.5
2
2.5
3
3.5
4
4.5
5
x (μm)
C, L=3 μm numerical
C1, L=3 μm analytical
C2, L=3 μm analytical
C3, L=3 μm analytical
C4, L=3 μm analytical

Figure 3

(a)

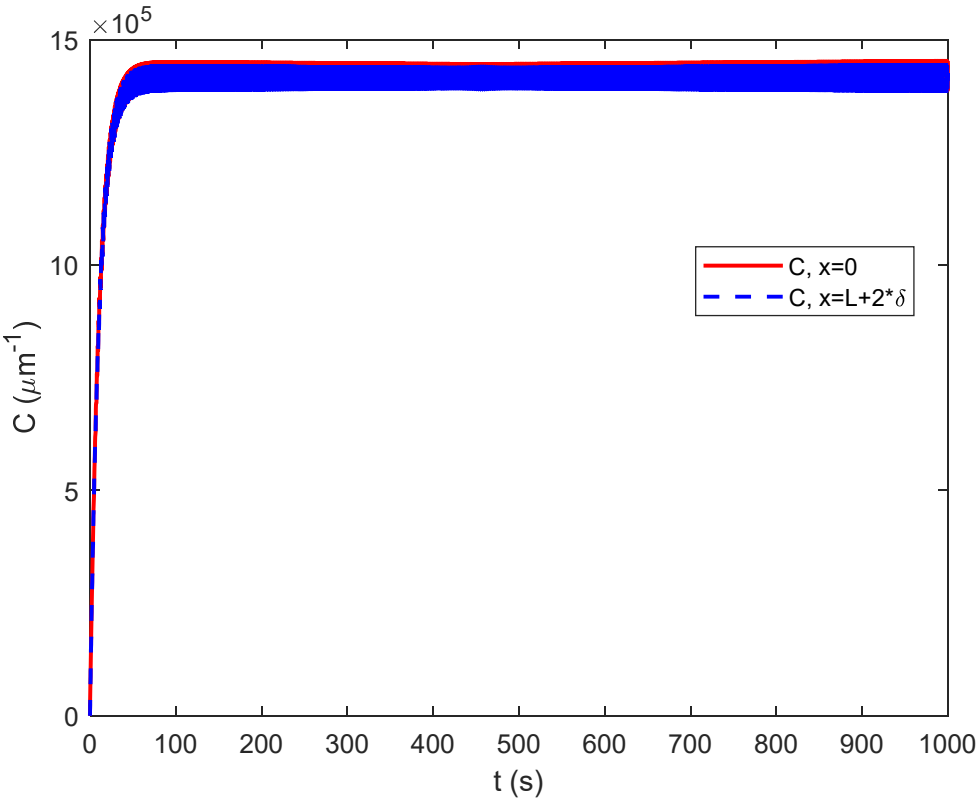

(b)

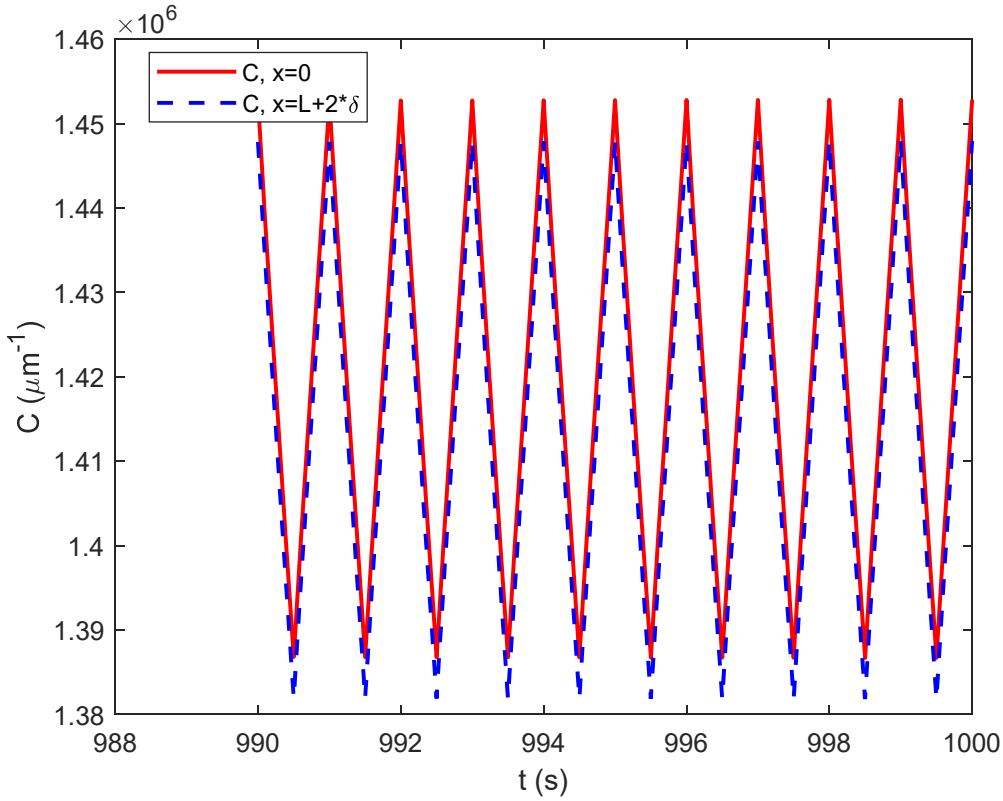

Figure 4a,b

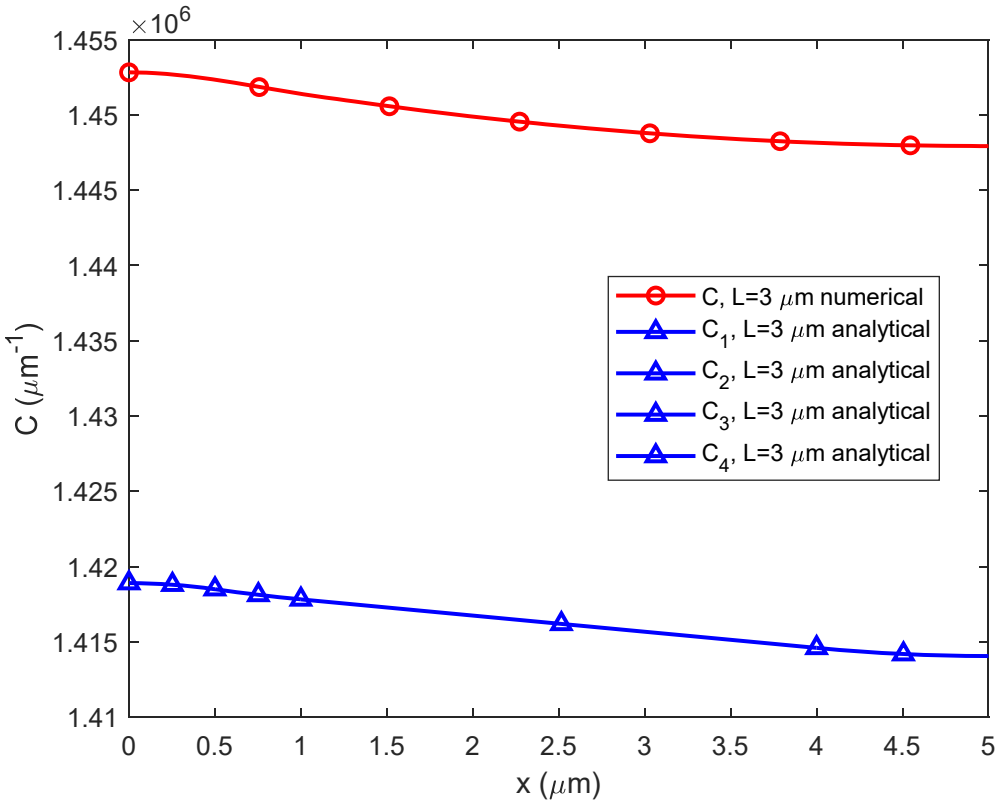
×10^6
1.455
1.45
1.445
1.44
1.435
1.43
1.425
1.42
1.415
1.41
C (μm^-1)
0
0.5
1
1.5
2
2.5
3
3.5
4
4.5
5
x (μm)
C, L=3 μm numerical
C1, L=3 μm analytical
C2, L=3 μm analytical
C3, L=3 μm analytical
C4, L=3 μm analytical

Figure 5

(a)

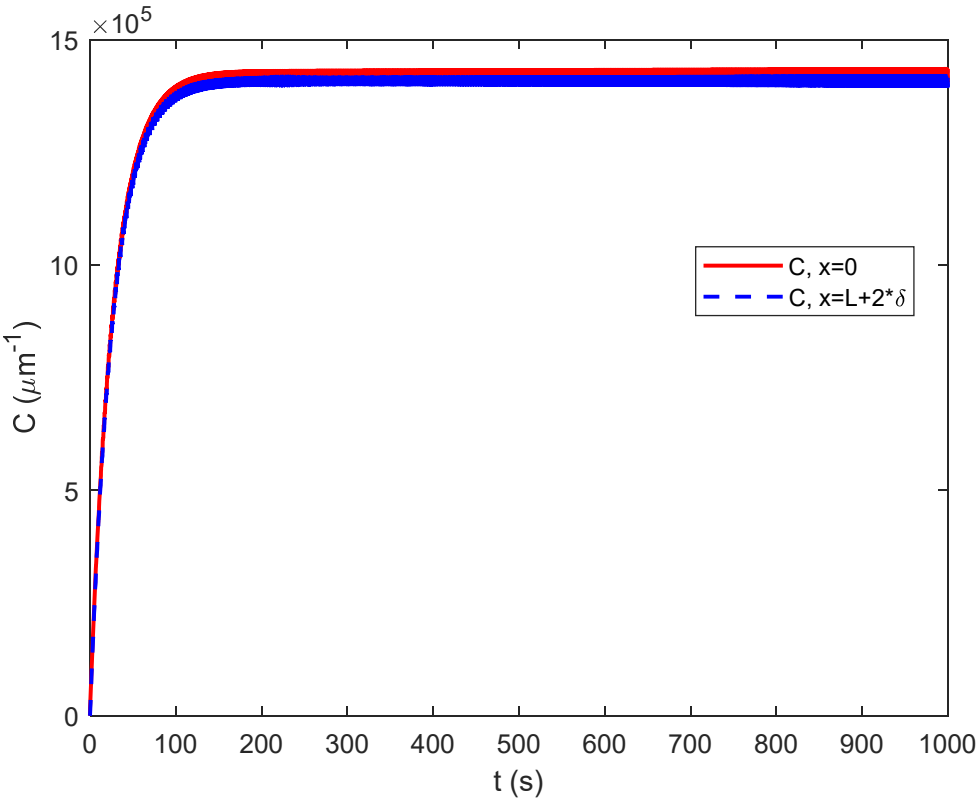

(b)

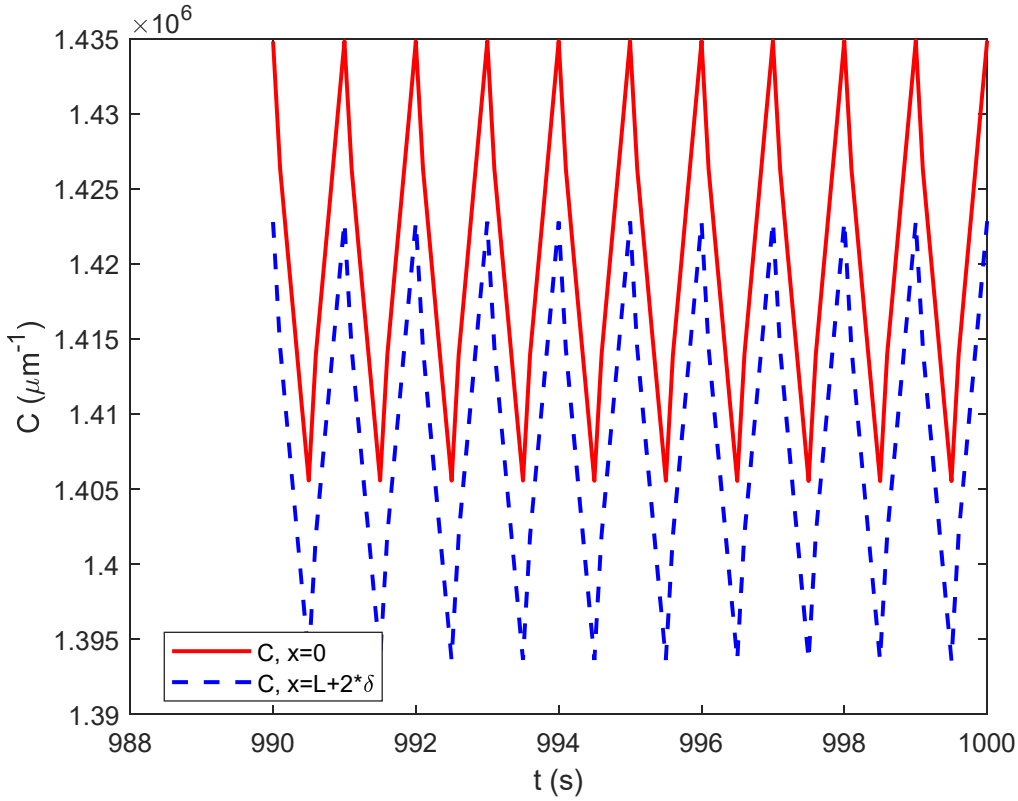

Figure 6a,b

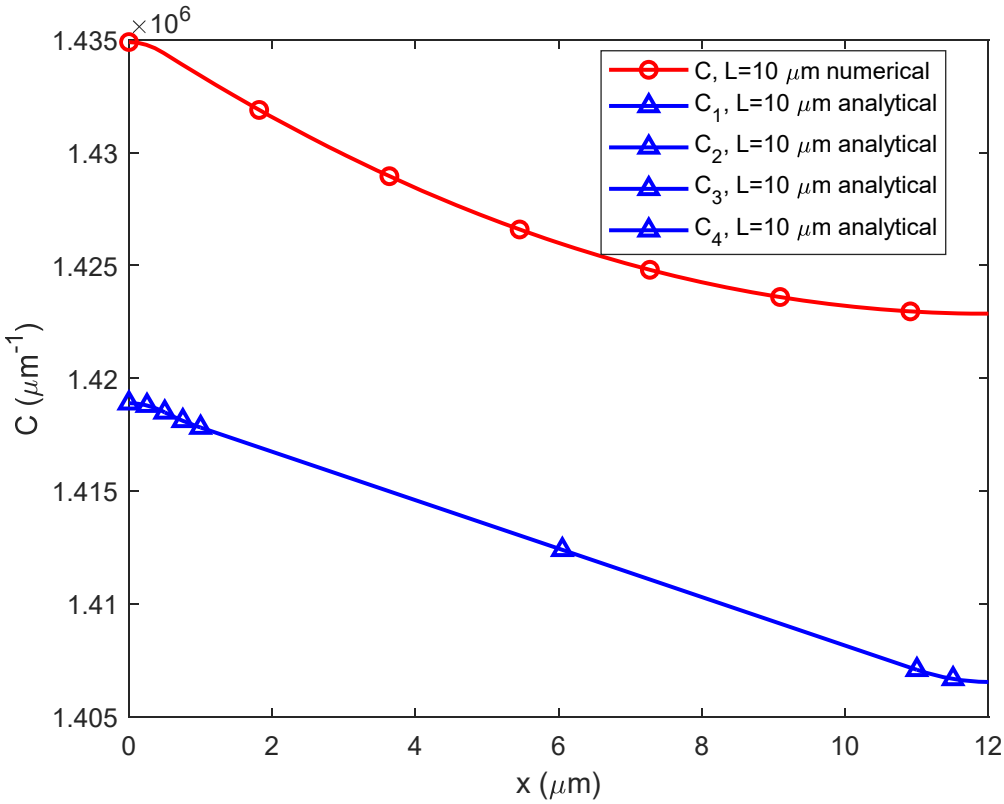
×10^6
1.435
1.43
1.425
1.42
1.415
1.41
1.405
C (μm^-1)
0
2
4
6
8
10
12
x (μm)
C, L=10 μm numerical
C1, L=10 μm analytical
C2, L=10 μm analytical
C3, L=10 μm analytical
C4, L=10 μm analytical

Figure 7

Effects of time-dependent ATP consumption caused by neuron firing on ATP concentrations in synaptic boutons containing and lacking a stationary mitochondrion

Andrey V. Kuznetsov

Department of Mechanical and Aerospace Engineering, North Carolina State University,

Raleigh, NC 27695-7910, USA; e-mail: avkuznet@ncsu.edu

Supplementary Materials

S1. Analytical solutions of governing equations obtained in ref. [19]

The analytical solution for Eqs. (1)-(4) with boundary conditions (6)-(10) for a constant rate of energy consumption in boutons ($a = a_0$) at steady-state is given by the following equations:

$$C_1(x) = -\left[m\left(\coth\left(\frac{\delta\sqrt{a}}{\sqrt{D}} \right) - 1 \right) \exp\left(-\frac{\sqrt{a}\left(2\delta + 2L + x + x_m\right)}{\sqrt{D}} \right) \right.$$

$$\times \left\{ 2\sqrt{D}\left[-\exp\left(\frac{2\sqrt{a}\left(\delta + L + x + x_m\right)}{\sqrt{D}} \right) + 2\exp\left(\frac{\sqrt{a}\left(2\delta + 2L + x + x_m\right)}{\sqrt{D}} \right) - 2\exp\left(\frac{\sqrt{a}\left(6\delta + 2L + x + x_m\right)}{\sqrt{D}} \right) \right.\right.$$

$$\left. + \exp\left(\frac{2\sqrt{a}\left(3\delta + L + x\right)}{\sqrt{D}} \right) - \exp\left(\frac{2\sqrt{a}\left(\delta + L + x_m\right)}{\sqrt{D}} \right) + \exp\left(\frac{2\sqrt{a}\left(3\delta + L\right)}{\sqrt{D}} \right) \right]$$

$$+ L\sqrt{a}\left(\exp\left(\frac{2\delta\sqrt{a}}{\sqrt{D}} \right) - 1 \right) \exp\left(\frac{2\sqrt{a}\left(\delta + L\right)}{\sqrt{D}} \right) \left[-2\exp\left(\frac{\sqrt{a}\left(2\delta + x + x_m\right)}{\sqrt{D}} \right) + \exp\left(\frac{2\sqrt{a}\left(\delta + x\right)}{\sqrt{D}} \right) + \exp\left(\frac{2\delta\sqrt{a}}{\sqrt{D}} \right) \right.$$

$$\left.\left.\left. + 2\exp\left(\frac{\sqrt{a}\left(x + x_m\right)}{\sqrt{D}} \right) - \exp\left(\frac{2\sqrt{a}\left(x + x_m\right)}{\sqrt{D}} \right) - \exp\left(\frac{2x_m\sqrt{a}}{\sqrt{D}} \right) \right] \right\} \right]$$

$$\left. \times \left[4a\left(\exp\left(\frac{2\delta\sqrt{a}}{\sqrt{D}} \right)\left(L\sqrt{a} + 2\sqrt{D} \right) - L\sqrt{a} + 2\sqrt{D} \right) \right]^{-1}, \qquad \text{(S1)}$$

$$C_2(x) = \left[m\left(\exp\left(\frac{2xm\sqrt{a}}{\sqrt{D}} \right) - 1 \right)\left(2\sqrt{D}\left(\exp\left(\frac{2\sqrt{a}\left(\delta + L + x\right)}{\sqrt{D}} \right) + \exp\left(\frac{2\sqrt{a}\left(3\delta + L\right)}{\sqrt{D}} \right) \right) \right) + \sqrt{a}L\left(\exp\left(\frac{2\delta\sqrt{a}}{\sqrt{D}} \right) - 1 \right) \right.$$

$$\times\exp\left(\frac{2\sqrt{a}\left(\delta+L\right)}{\sqrt{D}}\right)\left(\exp\left(\frac{2\delta\sqrt{a}}{\sqrt{D}}\right)+\exp\left(\frac{2x\sqrt{a}}{\sqrt{D}}\right)\right)\exp\left(-\frac{\sqrt{a}\left(4\delta+2L+x+x_m\right)}{\sqrt{D}}\right)\Bigg]$$

$$\times\left[8\left(a^{3/2}L\sinh^2\left(\frac{\delta\sqrt{a}}{\sqrt{D}}\right)+a\sqrt{D}\sinh\left[\frac{2\delta\sqrt{a}}{\sqrt{D}}\right]\right)\right]^{-1}, \tag{S2}$$

$$C_3\left(x\right)=\frac{m\left(\sinh\left(\frac{\delta\sqrt{a}}{\sqrt{D}}\right)\right)^{-1}\sinh\left(\frac{xm\sqrt{a}}{\sqrt{D}}\right)\left(\sqrt{D}\coth\left(\frac{\delta\sqrt{a}}{\sqrt{D}}\right)+\sqrt{a}\left(\delta+L-x\right)\right)}{a^{3/2}L+2a\sqrt{D}\coth\left(\frac{\delta\sqrt{a}}{\sqrt{D}}\right)}, \tag{S3}$$

$$C_4\left(x\right)=\frac{m\sqrt{D}\left(\exp\left(\frac{2xm\sqrt{a}}{\sqrt{D}}\right)-1\right)\left(\exp\left(\frac{2\sqrt{a}\left(2\delta+L\right)}{\sqrt{D}}\right)+\exp\left(\frac{2x\sqrt{a}}{\sqrt{D}}\right)\right)\exp\left(-\frac{\sqrt{a}\left(2\delta+L+x+xm\right)}{\sqrt{D}}\right)}{4\left(a^{3/2}L\sinh^2\left(\frac{\delta\sqrt{a}}{\sqrt{D}}\right)+a\sqrt{D}\sinh\left(\frac{2\delta\sqrt{a}}{\sqrt{D}}\right)\right)}. \tag{S4}$$

S2. Supplementary figures

(a)

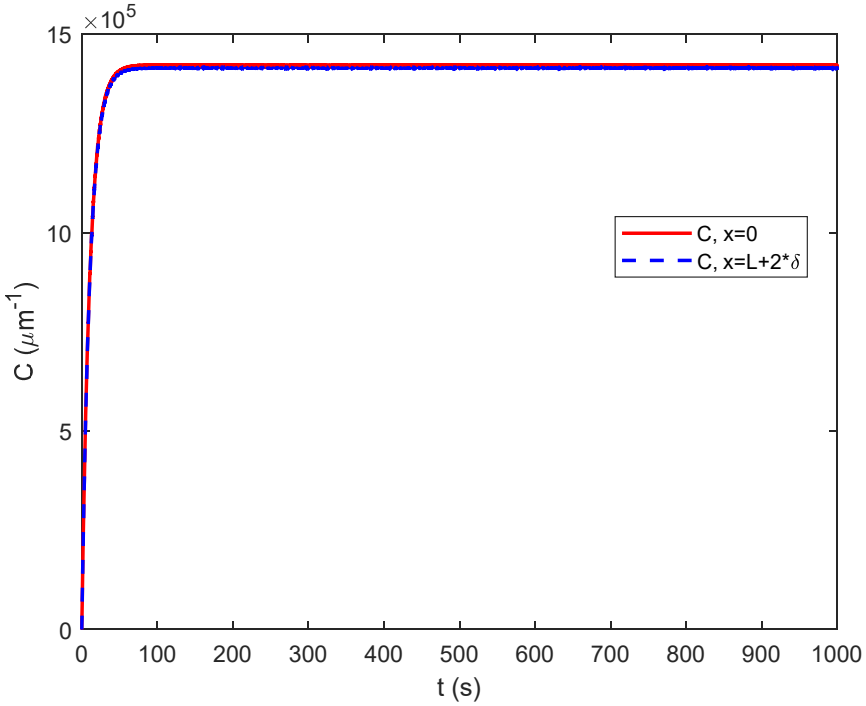

(b)

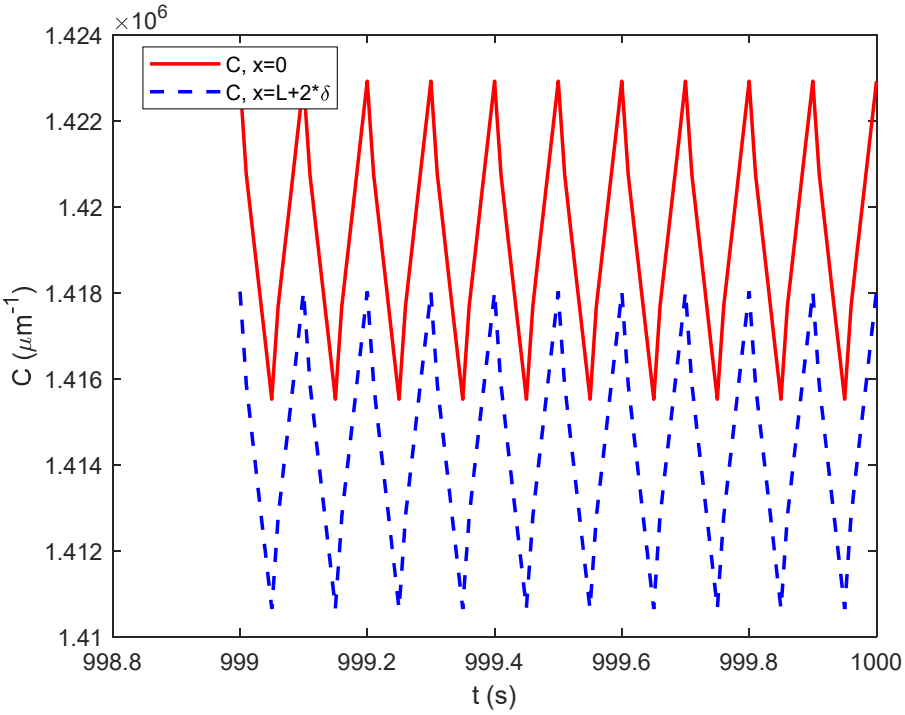

Fig. S1. Variation with time of the linear ATP concentration at x=0 (at the center of a bouton with a stationary mitochondrion) and at $x = L + 2\delta$ (at the center of a bouton without a stationary

mitochondrion). (a) The simulation covers the entire 1000 s. (b) The last 1 s of the simulation. f=10 Hz, L=3 μm.

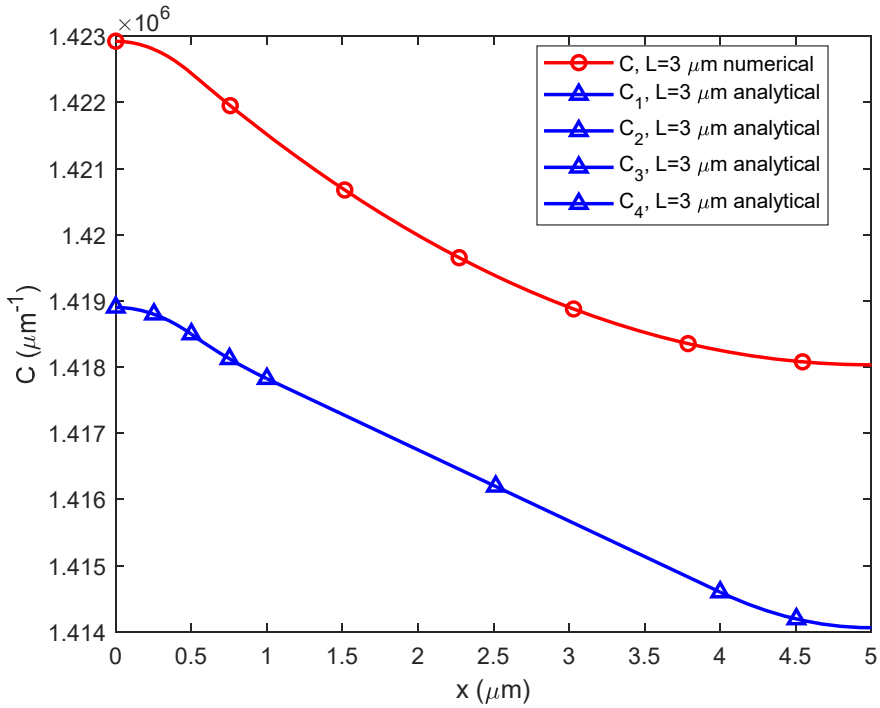

Fig. S2. The variation of ATP concentration between the centers of two boutons, one containing a stationary mitochondrion (at x=0) and the other without a stationary mitochondrion (at $x = L + 2\delta$), at t=1000 s. f=10 Hz, L=3 μm. The numerical solution represents the case with oscillating ATP consumption (as per Eq. (5)), whereas the analytical solution corresponds to the scenario with constant ATP consumption, a_0 (given in Table 1).

(a)

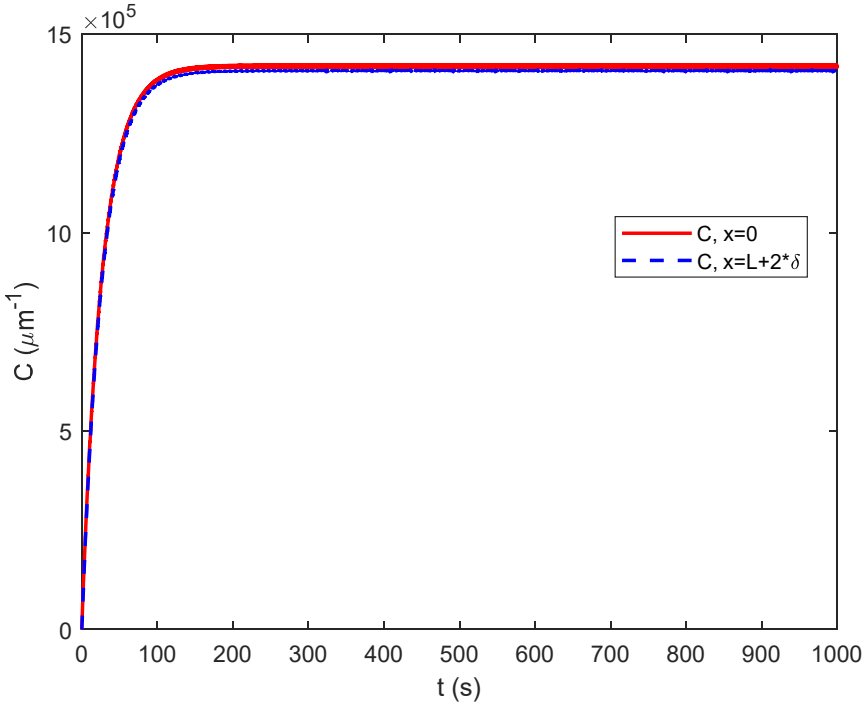

(b)

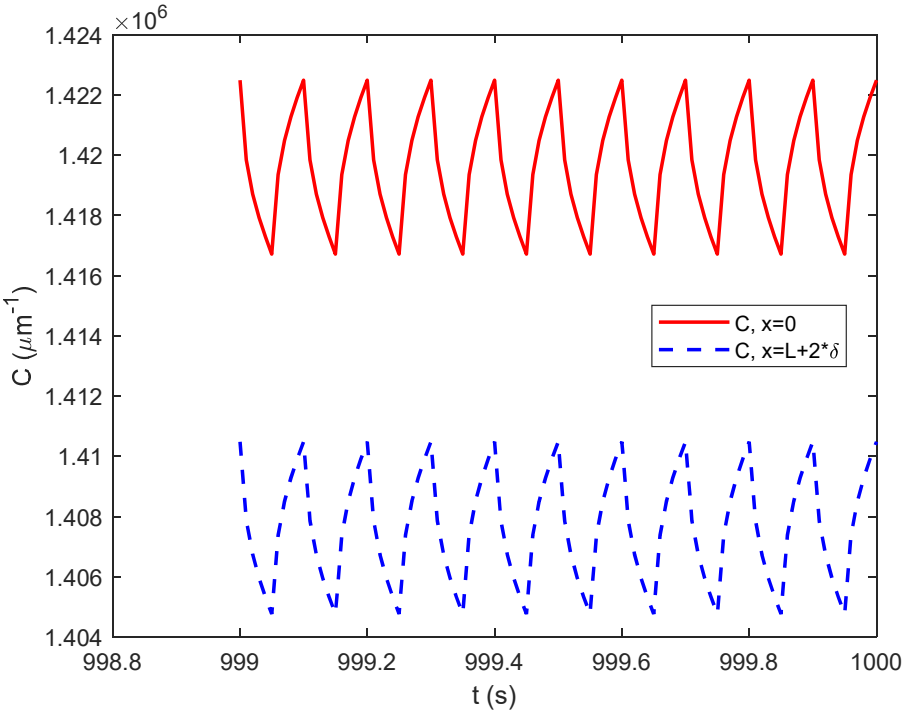

Fig. S3. Variation with time of the linear ATP concentration at x=0 (at the center of a bouton with a stationary mitochondrion) and at $x = L + 2\delta$ (at the center of a bouton without a stationary

mitochondrion). (a) The simulation covers the entire 1000 s. (b) The last 1 s of the simulation. f=10 Hz, L=10 μm.

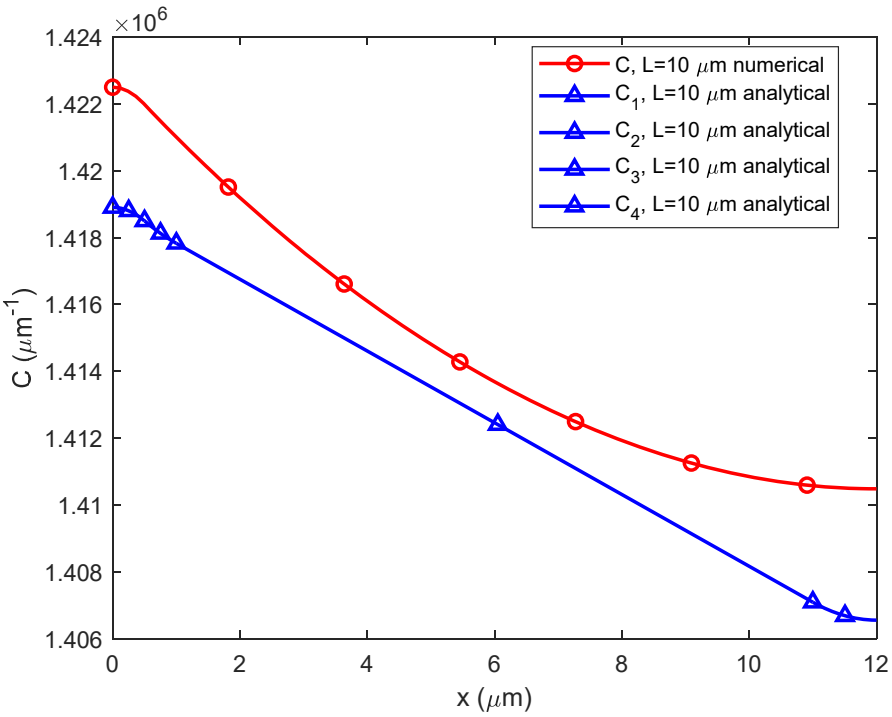

Fig. S4. The variation of ATP concentration between the centers of two boutons, one containing a stationary mitochondrion (at x=0) and the other without a stationary mitochondrion (at $x = L + 2\delta$), at t=1000 s. f=10 Hz, L=10 μm. The numerical solution represents the case with oscillating ATP consumption (as per Eq. (5)), whereas the analytical solution corresponds to the scenario with constant ATP consumption, a_0 (given in Table 1).